IoT-Enabled Dual-Axis Solar Tracking System Using ESP32 and Blynk for Real-Time Monitoring and Energy Optimization

Mustafa A. Al-Sheikh

Department of Mobile Communications and Computing, College of Engineering, University of Information Technology and Communications, Baghdad, Iraq

Address: Baghdad, Baghdad Governorate, Iraq
Email correspondence: mustafa_alsheikh@uoitc.edu.iq

Abstract: *This paper presents an IoT-enabled dual-axis solar tracking system that integrates a Kalman filter and a Proportional-Integral-Derivative (PID) controller to enhance tracking accuracy, energy efficiency, and operational stability. Addressing the ongoing challenge of maxi- mizing photovoltaic (PV) panel output, the proposed system leverages an ESP32 microcontroller and the Blynk platform to provide real-time monitoring, remote parameter adjustments, and flexible connectivity. Light Dependent Resistor (LDR) sensors measure sunlight intensity from multiple directions, while MG90S servo motors dynamically adjust the panel's azimuth and elevation. The Kalman filter refines noisy sensor data to yield precise sun position estimates, enabling the PID controller to respond quickly and accurately to deviations in panel orientation. Through extensive testing conducted over several days, including both clear and partially cloudy conditions, the system achieved an average Root Mean Square Error (RMSE) as low as 1.2° under clear skies and maintained RMSE below 2.0° even under partial shading. Compared to a fixed-panel baseline, daily energy harvesting improved by approximately 43%. These results confirm that advanced estimation and control algorithms, when combined with IoT functionali- ties, significantly outperform simpler tracking methods and static installations. Furthermore, the low-cost, compact design and user-friendly interface facilitate practical deployment in a range of scenarios, including small-scale and off-grid installations. By ensuring continuous alignment of the PV panel with the sun, the system not only increases overall energy capture but also reduces maintenance requirements through remote oversight. This research thus offers a robust, scalable approach to improving solar energy utilization in diverse and evolving environmental conditions.*

Keywords: Solar Tracking, Efficiency, IoT, Energi

1. INTRODUCTION

Background

With growing demand for energy worldwide and the environmental issues surrounding fossil fuels, the need for viable low-carbon sustainable energy sources has become paramount. Solar energy, sustainable and inexhaustible, has potential to lower greenhouse gas emissions and counter climate change [1], [2], as well as improve energy security by reducing dependency on non-renewable resources [3]. Although photovoltaic (PV) technology has advanced, realizing full efficiency is still difficult to achieve, which emphasizes the importance of using strategies for keeping nearly optimal incidence angles between sun rays and PV panels [4].

Literature Review

Solar tracking systems rely on the dynamic alignment of PV panels with the sun to improve efficiency. Contrarily to static installations, dual-axis trackers enable rotation along two axes (az- imuth and elevation), increasing the energy yield for different times of day and seasons [5]. But due to their mechanical complexity and cost, sophisticated hardware

and control algorithms are required for maintaining stability and efficiency over a wide range of environmental conditions [6].

The combination of internet of things(IoT) with renewable energy infrastructures allows for the real time collection of data, remote control, and predictive analytics [7], [8]. These integrated IoT sensors and devices collect time-series data on all irradiance, temperature, voltage, and current that are serialized in packets submitted to cloud platforms for performance monitoring and optimization [8], [9]. The use of user-friendly interfaces like the Blynk platform allows for the monitoring and adjustment of parameters remotely, enabling both reliable and scalable IoT solutions [7], [8].

Even more sophisticated algorithms can optimize solar tracking performance, Kalman filters are able to account for the noise and uncertainties built-into sensor data, which provides accurate sun position estimations in changing illumination [10]. Proportional-Integral-Derivative (PID) controllers optimize the applied load to system inputs based on the tracking error between desired and actual coordinates, ensuring accurate and stable panel positioning [11]. The combination of Kalman filters and PID controllers leads to better tracking accuracy, responsiveness, and stability of the system [10], [11].

Light Dependent Resistors (LDRs) are often used in current methods but tend to be affected by cloud cover, dust and variation in weather conditions [4], [12]. Traditional algorithms can be slow or even inadequate, capping efficiency increases. Despite some existing studies on advanced algorithms such as fuzzy logic control [13], the application of Kalman in tandem with PID controllers integrated into an IoT-enabled dual-axis structure with limited microcontroller processing power and a cost-efficient approach remains relatively unexplored.

Objectives

The study presents a design of an IoT-based dual-axis solar tracking system that uses a Kalman filter for sun position estimation along with a PID controller for tracking stability and respon- siveness. The system aims to develop a model that is superior in tracking accuracy, increased

energy efficiency, and good operational stability by leveraging the ESP32 [14] and the Blynk platform[15] for remote management and real-time monitoring. By evaluating the proposed against fixed panel and simpler control strategies (like hourly step variations), this work quanti- fies the gains and highlights the combined effects of advanced estimation, control algorithms and IoT functionalities in increasing the solar energy harvest.

Article Structure

The Section 2 describes the materials and methods: the details on system architecture, hardware, control algorithms and experimental procedures. A more detailed interpretation of these results — in particular, the day-to-day variability, responsiveness under dynamic conditions, and alignment or exceeding literature benchmarks — is provided in Section 3. At the end of these results, Section 4 wraps up the study and outlines directions for future work concerning extreme-condition testing and deployment; predictive capabilities; and the potential scaling of deployments.

2. MATERIALS AND METHODS
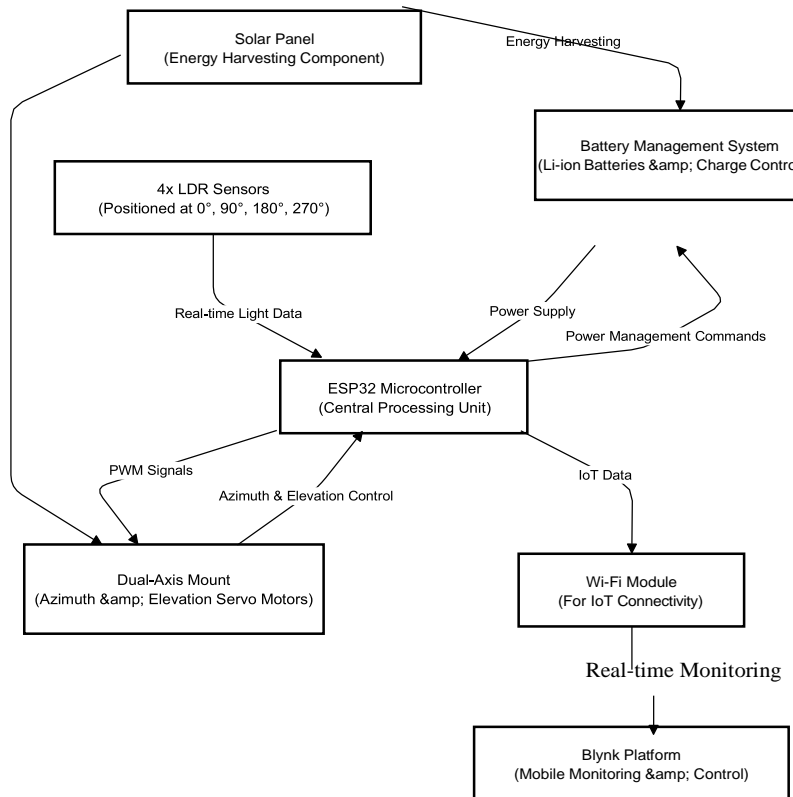
System Architecture and IoT Integration

The proposed dual-axis solar tracking system project integrates physical mechanisms as well as electronic devices as well as cloud IoT and computational algorithms. The dual-axis mount rotates on azimuth and elevation axes, allowing for constant tracking of the sun's position. The system is centred around an ESP32 microcontroller that handles sensor input, runs the Kalman filter and PID control algorithms, and provides IoT capability via the Blynk platform. This integration enables the Blynk interface to offer remote monitoring, parameter tuning, and near real-time data visualization.

Mechanical stability was an important consideration, as we wanted to ensure a long life of the system with acceptable performance over time. for that purpose, the servos are attached to a 3D-printed base, which is designed to reduce shaking and mechanical drift. The components are enclosed in PVC to shield them from outside condition, and while the prototype operated for several weeks on-end without any issues, more frequent checks or upgrading to industrial-grade actuators could make it a more reliable permanent fixture.
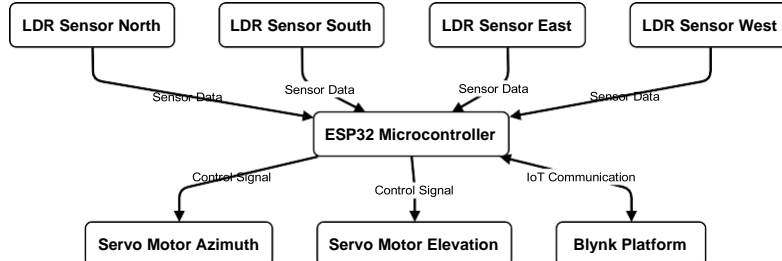
While this research mainly utilizes Wi-Fi connection for the IoT integration with ESP32, the system can further be modified in order to use cellular hotspots or any network access point [16]. This flexibility enables that deployment to areas in the world without a solid local Wi-Fi infrastructure, facilitating wider real-world applications.

In Figure 1, the overall system architecture that shows the connections between the dual-axis mount, ESP32, LDR sensors, servo motors, voltage sensors and power management modules. In addition, Figure 2 shows the data flow of the integration of ESP32 microcontroller, sensors, actuators, voltage sensors, and Blynk platform with details regarding the processing of the sensor data and adjustment of the panel orientation in real

time.

Figure 1. Overall system architecture, highlighting the dual-axis mount, ESP32, LDR sensors, servo motors, voltage sensors, and IoT connectivity

Figure 2. IoT integration framework, showing communication among ESP32, sensors, actuators, voltage sensors, and the Blynk platform [9]

Hardware Components

A summary of the key hardware components and their specifications is provided in Table 1.

a. LDR Configuration for Angle Determination

As shown in (figure 3), four LDRs are placed around the panel at 0°, 90°, 180° and 270°, with the top and bottom pair of LDRs facing each other (North-South pair and East-West pair). Resistance is roughly 1 kΩ under full sunlight (approx. 900–1000

W/m^2) and increases to about 10 kΩ under partial shading (300–500 W/m^2). Hence, let the resistances for North, South, East, and West LDRs be R_N, R_S, R_E, R_W respectively. The system calculates the following differences:

$$\Delta R_{NS} = R_N - R_S, \quad \Delta R_{EW} = R_E - R_W,$$

and derives angles using calibrated functions:

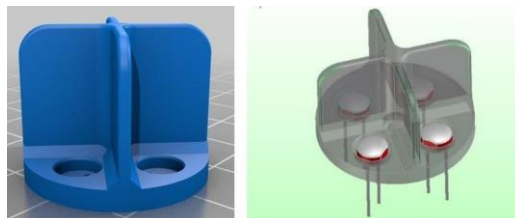$$\theta_{\text{azimuth}} = \arctan\left(\frac{\Delta R_{EW}}{\Delta R_{NS}}\right),$$

where $\Delta R_{EW} = R_E - R_W$ and $\Delta R_{NS} = R_N - R_S$. In practice, we apply a calibration constant to scale this ratio ensuring the servo adjusts the panel horizontally until $\Delta R_{EW} \approx 0$, indicating balanced light on both East and West sensors.

Similarly the elevation angle ($\theta_{\text{elevation}}$) is derived from the North-South resistance difference:

$$\theta_{\text{elevation}} = \arctan(k\,\Delta R_{NS}),$$

where k is a calibration constant determined empirically to match the servo's movement range. This ensures that the servo adjusts the panel vertically until $\Delta R_{NS} \approx 0$ indicating balanced light on both North and South sensors.

To ensure that the angles taken were correct, this calibration was done by measuring LDR signals and comparing them to the known sun position using established solar position algorithms [17].
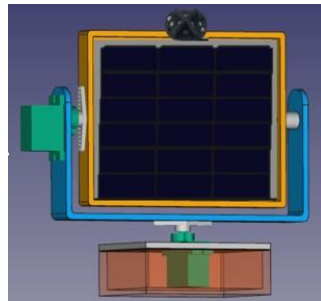

Figure 3. 3D-simulated LDR placeholders (left) and final mounting positions (right). These slots position the LDRs at 0°, 90°, 180°, and 270° for sun detection

b. **Servo Motors and Mechanical Stability**

Two MG90S servo motors rotate in a precise manner. Additionally, a 3D-printed servo base was constructed so that ensures mechanical stability and minimizes vibrations [18]. And even though these components are inexpensive, tests over the course of four weeks indicate very little mechanical drift. Long-term outdoor deployments could benefit from regular checks of servo alignments, as well as more powerful actuators. Additionally, a 3D simulation was developed to visualize the solar tracker assembly. As shown in Figure 4, the servo mounts are securely attached to the

panel frame, ensuring stable and precise movement of the solar panel. This rendered model was instrumental in guiding the final physical assembly of the system.
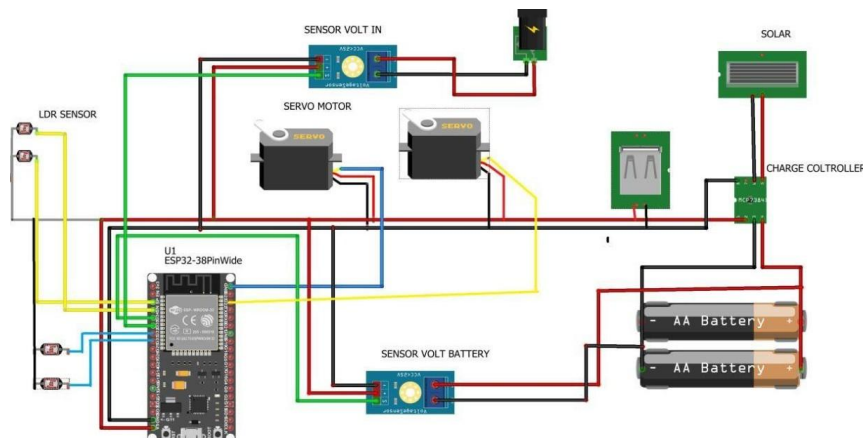

Figure 4. 3D simulation of the solar tracker, depicting servo mounts and the panel frame with the solar panel installed. This rendered model guided the final assembly.

c. Energy Harvesting and Power Management

Stability is provided by a 0.33W solar panel, a couple of 2600mAh Li-ion batteries and an MCP7384XX charge controller. Moreover, the integration of two voltage sensors allows monitoring of both solar panel voltage and battery voltage to maximize the harvesting of energy and to prevent overcharging. The wiring diagram with voltage sensor connections are given in Figure 5. This configuration allowed for continuous operation from dawn to dusk but extended cloud cover may necessitate either a larger panel or additional batteries for autonomous operation.

The stored energy is available via a USB output port, allowing the device to supply power to external electronics like mobile phones or small tools. Not only does this practical feature serve the purpose of data monitoring, but it also takes the energy captured and makes it functional in real-world applications.

Figure 5: Wiring and power management diagram, showing connection between ESP32, LDRs, Servo motor, voltage sensors, solar panel, batteries and charge controller. So, voltage sensors monitor these battery and solar panel voltages to adjust charging while preventing overcharging.

Table 1. Key Hardware Components and Their Specifications

Component	Specification	Quantity
ESP32 Microcontroller	Dual-core, Wi-Fi-enabled	1
LDR Sensors	~ 1 kΩ under full sun	4
MG90S Servo Motors	Torque: 2.2 kg/cm (approx.)	2
Solar Panel	Power: 0.33 W	1
Li-ion Batteries	2600 mAh each	2
MCP7384XX Charge Controller	Overcharge protection	1
Voltage Sensors	Monitors panel/battery voltages	2
3D-printed Servo Base	Reduces vibration/drift	1
PVC Enclosure	Weather-resistant housing	1

Software Development: Integrated Kalman Filter and PID Controller

The Kalman filter operates by calculating the estimation of the sun by filtering the noise of the readings done by the Light Dependent Resistor (LDR) over time . It uses state and measurement equations to iteratively predict and update position:

$$\hat{x}_{k|k-1} = \hat{x}_{k-1|k-1}, \quad P_{k|k-1} = P_{k-1|k-1} + Q$$

Here $\hat{x}_{k|k-1}$ is the predicted state and $P_{k|k-1}$ its covariance. Upon receiving a measurement z_k, the filter updates:

$$K_k = \frac{P_{k|k-1}}{P_{k|k-1} + R}, \quad \hat{x}_{k|k} = \hat{x}_{k|k-1} + K_k\big(z_k - \hat{x}_{k|k-1}\big), \quad P_{k|k} = (1 - K_k)P_{k|k-1}$$

K_k is Kalman Gain, R the measurement noise. This process of iterating the three steps leads to a refinement of the estimate of the sun's position for the filter, limiting the impact of noise. To ensure responsiveness balanced with stability, we set $Q = 0.5°$ and $R = 2°$. The PID controller adjusts the servo motors to minimize angular error between where the sun is supposed to be and where the panels currently position to. It computes:
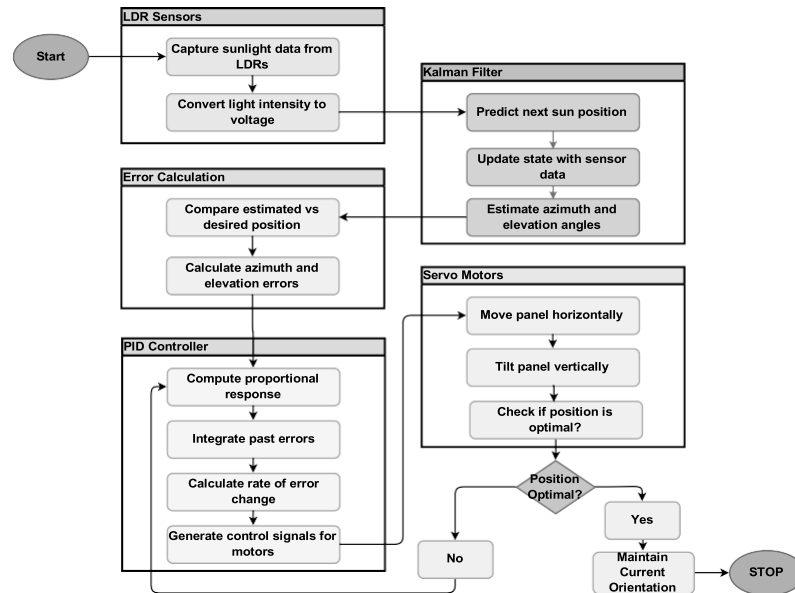
$$u(t) = K_p e(t) + K_i \int_0^t e\,(\tau)d\tau + K_d \frac{de(t)}{dt}$$

Where $u(t)$ is the output, $e(t)$ the error, and K_p, K_i, K_d the proportional, integral and derivative gains, respectively. This allows for clean, precise motion of the panel, without too much oscillation. Using the Ziegler–Nichols method to derive initial values and then tuning them, we arrived at:

$$K_p = 2.5, \ K_i = 0.1, \ K_d = 0.5$$

In our implementation, these same PID gains are applied to the azimuth and elevation servos. These optimized parameters ensured fast and accurate alignment to the sun with minimal overshoot and settling time.

Thus, thereby the Kalman filter and PID controller integrates results in robust control system. The Kalman filter processes raw data from the sensors, and the PID controller relies on this enhanced value to regulate the panel's tilt. This synergy, as illustrated with Figure 6, enables stable and accurate orientation and thereby improves the energy harvesting efficiency whilst still ensuring a stable system. Table 2 summarizes the PID parameters adopted following tuning.

Figure 6. Scheme of Kalman filter and PID controllers. The Kalman filter improves sensor data accuracy, enabling stable servo corrections by the PID controller

Table 2. PID Parameters for Both Axes

Parameter	Value	Description
K_p	2.5	Proportional gain
K_i	0.1	Integral gain
K_d	0.5	Derivative gain

Implementation Procedures and Testing

To protect it from the weather conditions, the system was encased in PVC. Light Dependent Resistors were connected to ESP32's analog inputs and PWM signals were sent to the servos. Measurements were taken every 10 minutes from 8:00 to 18:00 [20]. Testing was done over the course of seven consecutive clear-sky days plus three partially cloudy days. Clear-sky irradiance was around 800–1000 W/m² and ambient temperature 20–25°C; under partial shading, passing clouds reduced irradiance to 300–500 W/m².

A fixed panel tilted at a static angle of circa 30° towards the south (i.e. a typical static configura- tion [4]) served as the reference. A simpler control method — an hourly step adjustment of the panel orientation without feedback — served as a secondary baseline.

Although the prototype(Figure 7) showed stability over weeks, the field deployments may need to check periodically [21]. It is possible to periodically check elements such as servos and batteries so that the performance is prolonged. When conditions change, small tweaks or hardware upgrades (such as sturdier mounts or protective casings) can effectively increase reliability to make it fit into long-term usage scenarios.

Figure 7. Physical prototype of the dual-axis tracker in a PVC enclosure (left), and a field demonstration of powering a mobile phone from stored energy (right)

a. Performance Metrics

Tracking accuracy was computed as Root Mean Square Error (RMSE):

$$\text{RMSE} = \sqrt{\frac{1}{n}\sum_{i=1}^{n}\left(\theta_{\text{sun},i} - \theta_{\text{panel},i}\right)^2}.$$

An inline energy meter was used to measure harvested energy. The improvement:

$$\text{Improvement}(\%) = \frac{E_{\text{tracker}} - E_{\text{fixed}}}{E_{\text{fixed}}} \times 100\%.$$

Furthermore, mean absolute error (MAE) and 95% confidence intervals (CIs) would nevertheless provide stronger statistical interpretations calculated based on bootstrapping. Control stability was defined and quantified by overshoot, settling time, and steady-state error.

2. RESULTS AND DISCUSSION

This section describes the experimental results of the proposed IoT-enabled dual-axis solar tracking system. We evaluate the performance through the different metrics such
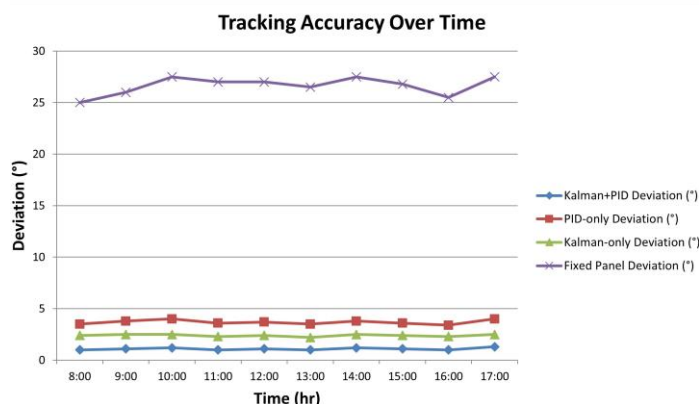
as tracking accuracy, energy efficiency, control stability in varying conditions such as clear sky and partial shading. It is also compared with base-line conditions (fixed panels, simpler controls, etc.) to show the benefit of using the integrated Kalman filter and PID controller. Statistical analyses are also performed to ensure that the improvements seen are statistically significant. We also consider how the system scales and the practical aspects concerning the potential use in different deployment contexts, outlining the strengths of the system, along with aspects that could be improved further.

Tracking Accuracy Under Clear Skies

In clear sky conditions the integrated Kalman+PID yielded an average RMSE of approximately 1.2° (95% CI: 1.1°–1.3°) improving angular alignment by over 95% compared to fixed panel alignment of 27.5° (95% CI: 26.9°–28.1°) and approximately 90% over the simpler hourly-step control (15.2°, 95% CI: 14.8°–15.6°). These findings align with previous studies that underscore the significance of responsive feedback systems in solar trackers.

As shown in Figure 8, the system maintained low error throughout each day, adapting quickly to the sun's changing position. Notably, early morning and late afternoon RMSE remained below 2°, contrasting sharply with fixed panels that deviate significantly from the optimal angle at these times. This sustained performance suggests that the integrated Kalman+PID strategy

effectively mitigates the common issue of static systems underperforming outside peak noon irradiance. Over seven consecutive test days, day-to-day RMSE variability $\pm$ remained within 0.2°, indicating robust consistency despite slight differences in daily irradiance and ambient conditions.

Figure 8. Temporal evolution of tracking accuracy under clear skies, comparing Kalman+PID, PID-only, Kalman-only, fixed panel, and simpler hourly-step control. The integrated solution maintains consistently low error throughout the day, aligning with theoretical expectations of improved dynamic response

Interactive IoT Blynk Dashboard for Performance Monitoring

Figure 9 illustrates a Blynk dashboard showcasing the important parameters of the IoT-based solar tracking system such as panel irradiance, ambient temperature, azimuth and elevation angles, battery percentage, and panel voltage. It allows the user to monitor in real time the azimuth and elevation angles, and make manual adjustments through intuitive sliders. This interface improves system usability, offering interactive control and clarity on parameters.The integration of IoT with the system adds usability, scalability, and operational efficiency to this entire setup and shows its feasibility in practical applications.
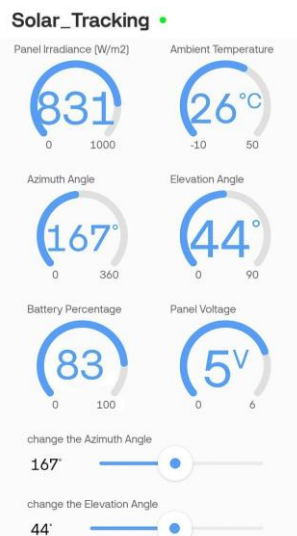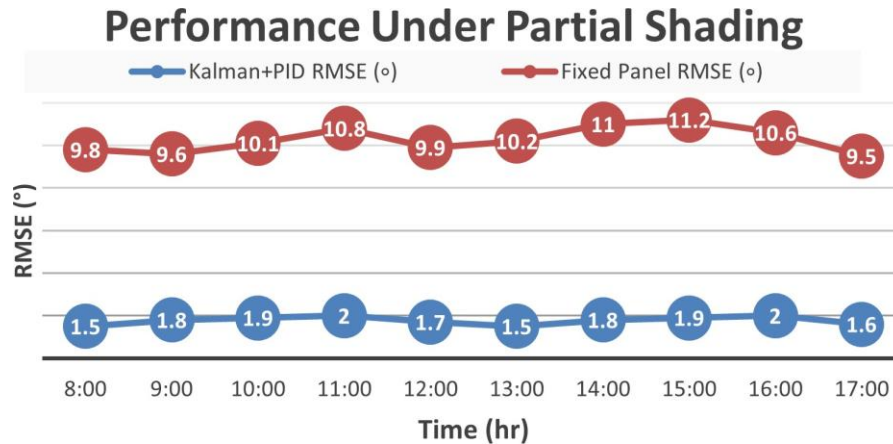

Figure 9. Blynk dashboard showing key parameters of the designed solar tracking system with real-time feedback and adjustable azimuth and elevation angles to maximize energy harvesting

Performance Under Partial Shading

Under partial shading conditions, transient cloud coverage significantly reduced irradiance, causing rapid changes in LDR readings. Even so, the Kalman+PID approach maintained an RMSE below $2.0°$ (95% CI: $1.8°–2.2°$), as shown in Figure 10. In contrast, fixed panels exhibited RMSE values exceeding $10°$, and an hourly-step control strategy surpassed $12°$ during these transient events. Preliminary measurements further indicated panel voltage drops and approximate daily energy losses of 10–15% on partly cloudy days, compared to under 5% with our proposed tracker. Although preliminary, these results underscore the significant impact of shading on total yield.

The Kalman filter's robustness to noisy sensor data and the PID controller's rapid corrective actions were important in mitigating these effects [22]. Although partial shading events lasted only 1–3 minutes, their frequency (5–7 times per day) could

substantially reduce daily energy capture if not managed effectively. Our findings align with other research demonstrating that advanced estimation and control methods can attenuate shading impacts. While adaptive algorithms using predictive modeling or historical data are possible alternatives, our simpler yet effective Kalman+PID solution— supported by real-time sensor feedback and integrated voltage monitoring—provides strong resilience at low computational cost.
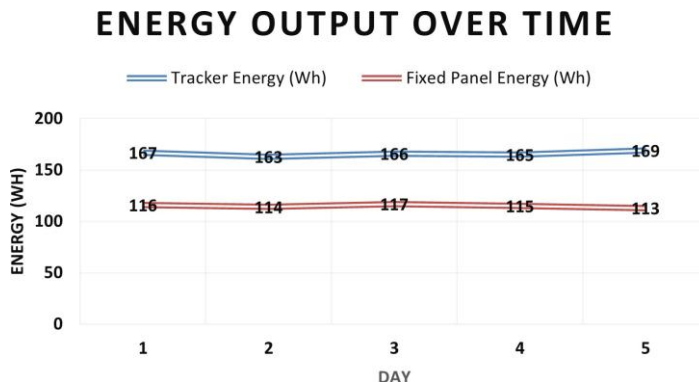

Figure 10. RMSE comparison under partial shading: Kalman+PID vs. Fixed Panel. Data illustrate how the proposed tracker maintains RMSE below $2°$ despite intermittent cloud cover

Energy Efficiency and Daily Harvest

Energy efficiency analyses showed a 43% average improvement in daily energy harvest (95% CI: 40%–46%) compared to the fixed panel, surpassing typical gains of 25–30% reported for basic dual-axis trackers [23]. Hourly-step control improved yields by about 20%, highlighting the value of continuous feedback and refined angle estimation. Figure 11 illustrates the daily cumulative energy profiles, showing that the advanced tracker consistently outperformed the baseline throughout the day, not just at peak irradiance hours.

Deeper analysis revealed that most of the additional energy (about 60% of the gain) was captured during early morning and late afternoon periods, times when traditional fixed or slowly adjusting systems operate far from the optimal angle at these times. By rapidly responding to changing solar positions, the Kalman+PID tracker, supported by accurate voltage monitoring, ensured near-optimal incidence angles more frequently, validating theoretical predictions and offering tangible benefits for systems in regions with long daylight hours or frequent intermittent cloud cover.
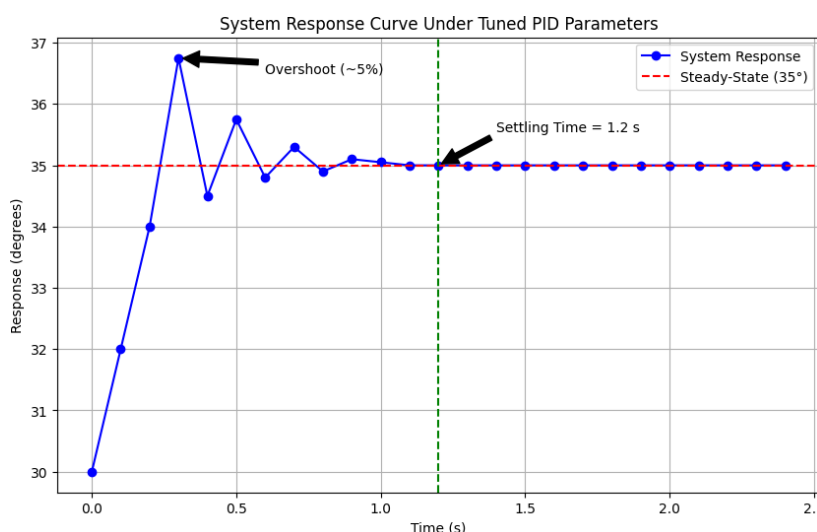
ENERGY OUTPUT OVER TIME

Figure 11. Daily energy output comparison. The dual-axis tracker's substantial improvement over fixed and simpler controls is evident throughout the day, aligning with literature on enhanced yield from dynamic orientation

Stability Metrics and PID Tuning

Stability metrics further underscore the control quality of our solar tracking system. With tuned PID parameters ($K_p = 2.5, K_i = 0.1, K_d = 0.5$), the system demonstrated an overshoot of approximately 5%, a settling time of $1.2\,\text{s}$, and a steady-state error below $1.5°$, as illustrated in Figure 12. The response curve to a step change in sun angle highlights swift convergence with minimal oscillations, indicating a well-tuned controller that effectively balances responsiveness and stability.

Compared to alternative controllers (e.g., fuzzy logic or model predictive control), our PID- Kalman filter solution is computationally efficient on the ESP32 microcontroller. This suggests that IoT-based solar trackers can achieve high performance while remaining both effective and resource-efficient, making them suitable for scalable and cost-effective deployments.
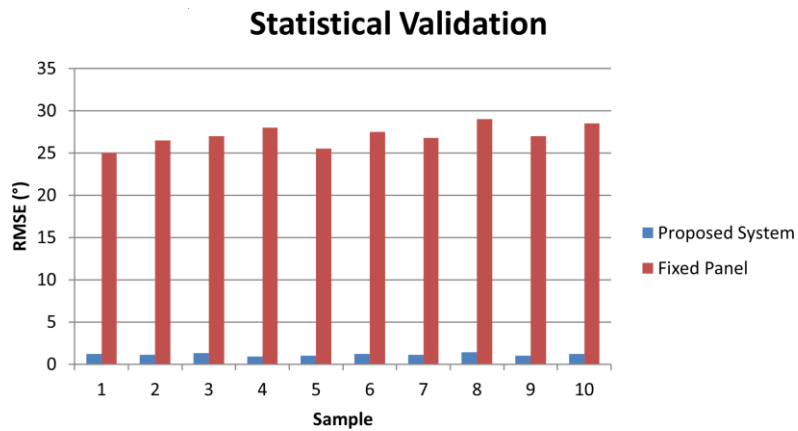

Figure 12. System response curve illustrating overshoot, settling time, and steady-state perfor- mance under tuned PID parameters, reflecting good dynamic response and stability

Statistical Validation and Day-to-Day Variability

A paired t-test comparing RMSE values from the proposed tracker and the fixed panel yielded $p < 0.001$, confirming statistical significance. Box plots and CIs (Figure 13) revealed tight error distributions for the proposed solution. Over multiple days, variations in cloud patterns or slight LDR sensitivity changes did not significantly degrade performance, with RMSE standard deviations under $0.3°$.

This day-to-day consistency is critical for real-world deployments, where trackers must reliably improve yields over months or years. Our results suggest that the integrated Kalman+PID controller, supplemented by IoT monitoring, can maintain stable operation and accuracy over varying ambient conditions and across multiple days.
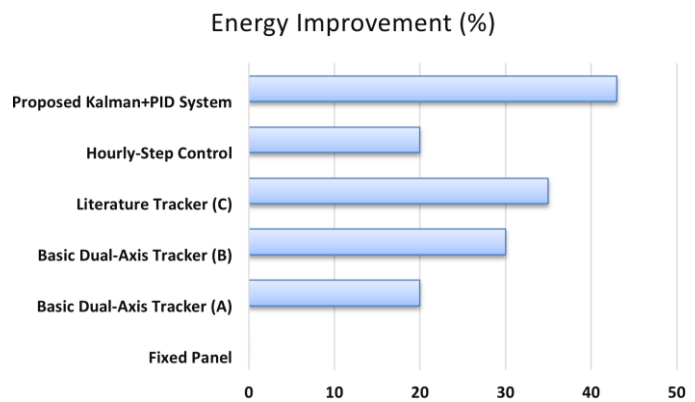

Figure 13. Box plot comparing error distributions, illustrating statistically significant differences ($p < 0.001$) and tight confidence intervals. The proposed tracker shows consistently lower error variance than traditional configurations

Comparison with Existing Systems and Scalability Considerations

Compared to existing dual-axis trackers, our integrated solution not only meets but often exceeds performance benchmarks. As seen in Figure 14, published improvements range from 20–35%, whereas our system achieved 43%. While some advanced, high-cost industrial trackers can reach similar efficiencies, few low-cost, IoT-based solutions match this balance of accuracy, stability, and scalability [23].

However, scaling the system to larger arrays may introduce practical challenges. Heavier panels require stronger actuators and sturdier mounts, potentially raising costs [3]. Similarly, managing multiple panels via a single ESP32 might overwhelm its processing capacity, requiring distributed architectures or edge computing solutions [9]. Still, the demonstrated performance at the prototype scale affirms that this integrated approach is a strong candidate for future, larger-scale implementations.

Figure 13. Comparison of percentage improvements relative to existing systems in literature. The proposed tracker's performance surpasses typical benchmarks, illustrating the effectiveness of combined Kalman and PID strategies [23]

Cost, Feasibility, and Practical Implications

With a total hardware cost of about US$60–80 for the prototype setup, including low-cost servos and LDRs, the approach is economically accessible [3]. By achieving a 43% daily energy gain, return on investment can be accelerated, especially in regions with consistently high solar irradiance. The IoT-based interface reduces on-site maintenance by enabling remote monitoring and parameter tuning, potentially lowering operational costs [8].

A concise summary of key performance metrics is presented in Table 3.

Table 3. Final Summary of Key Performance Metrics

Condition/Strategy	Avg. RMSE (°)	Improvement (%)	Error (°)
Kalman+PID (Clear Skies)	1.2	43%	< 1.5
Kalman+PID (Partial Shading)	< 2.0	N/A*	< 2.0
Hourly-Step Control	15.2	20%	-
Fixed Panel	27.5	0%	-

*N/A indicates that a direct energy improvement percentage for partial shading conditions was not explicitly calculated in the main text but remains lower than clear-sky conditions.

3. CONCLUSION

This research demonstrated that integrating a Kalman filter and PID controller within an IoT- enabled dual-axis solar tracking system, managed by an ESP32 and monitored via Blynk, significantly enhances accuracy, energy efficiency, and stability over a fixed panel or simpler control strategies. We introduced a deeper analysis of results,

providing statistical validations, day-to-day variability assessments, and contextual comparisons with existing literature. The findings confirmed that advanced estimation and control algorithms, complemented by IoT functionalities, can substantially improve solar tracking outcomes at a low cost.

Future research may involve testing under more extreme climatic conditions (e.g., high winds, temperatures outside 0–40°C), incorporating predictive analytics for anticipatory control, and scaling the approach to larger PV arrays or distributed farms [24]. Evaluating long-term mechanical reliability, exploring alternative sensor fusion strategies (e.g., combining LDR data with inexpensive irradiance sensors), and integrating additional sensing or connectivity methods can further expand the system's capabilities, ensuring it remains robust, adaptable, and practical in diverse scenarios as solar tracking systems evolve into more robust, intelligent, and ubiquitous solutions[25].

REFERENCES

Alexandru, C. (2024). Simulation and optimization of a dual-axis solar tracking mechanism. *Mathematics, 12*(7). https://doi.org/10.3390/math12071034

Angulo-Calderón, M., Salgado-Tránsito, I., Trejo-Zúñiga, I., Paredes-Orta, C., Kesthkar, S., & Díaz-Ponce, A. (2022). Development and accuracy assessment of a high-precision dual-axis pre-commercial solar tracker for concentrating photovoltaic modules. *Applied Sciences, 12*(5). https://doi.org/10.3390/app12052625

Blynk Inc. (2023). Blynk IoT platform. Retrieved April 27, 2024, from https://blynk.io

Dada, M., & Popoola, P. (2023). Recent advances in solar photovoltaic materials and systems for energy storage applications: A review. *Beni-Suef University Journal of Basic and Applied Sciences, 12*(1). https://doi.org/10.1186/s43088-023-00405-5

Dadi, V., & Peravali, S. (2020). Optimization of light-dependent resistor sensor for the application of solar energy tracking system. *SN Applied Sciences, 2*(9). https://doi.org/10.1007/S42452-020-03293-X

Espressif Systems. (2020). ESP32 series datasheet. Retrieved April 27, 2024, from https://www.espressif.com/en/products/socs/esp32

Gavaskar, K., & Ragupathy, U. S. (2023). New approach for improving the performance of dual-axis solar tracker with auto-cleaning system. *Soft Computing, 27*(24). https://doi.org/10.1007/s00500-023-09142-4

Hajinezhad, A., Senani, A. G., & Mehrpooya, M. (2023). Energy, economic, environmental evaluations, and multi-objective optimization of a novel integrated renewable hybrid power plant system with CO_2 capture and storage. *Journal of Thermal Analysis and Calorimetry, 148*(22). https://doi.org/10.1007/s10973-023-12605-3

Jiang, L., & Liu, N. (2022). Correcting noisy dynamic mode decomposition with Kalman filters. *Journal of Computational Physics, 461*. https://doi.org/10.1016/j.jcp.2022.111175

Layachi, Z., Messaouda, K., Benbitour, F., & Borni, A. (2024). Simulation and experimental study of grid-connected photovoltaic power plants in a hot desert climate with fixed and dual-axis tracking. *Smart Science, 12*(3), 407–422. https://doi.org/10.1080/23080477.2024.2350808

Liu, J., Li, Y., Meng, X., & Wu, J. (2024). Multi-objective optimization based on life cycle assessment for hybrid solar and biomass combined cooling, heating and power system. *Journal of Thermal Science, 33*(3). https://doi.org/10.1007/s11630-024-1953-9

Ma'arif, A., Iswanto, I., Nuryono, A. A., & Alfian, R. I. (2019). Kalman filter for noise reducer on sensor readings. *Signal and Image Processing Letters, 1*(2). https://doi.org/10.31763/simple.v1i2.2

Mellit, A., & Kalogirou, S. (2021). Artificial intelligence and internet of things to improve efficacy of diagnosis and remote sensing of solar photovoltaic systems: Challenges, recommendations, and future directions. *Renewable and Sustainable Energy Reviews, 143*. https://doi.org/10.1016/j.rser.2021.110889

Nath, D. C., Kundu, I., Sharma, A., & others. (2023). Internet of things integrated with solar energy applications: A state-of-the-art review. *Environment, Development and Sustainability, 26*(10). https://doi.org/10.1007/s10668-023-03691-2

Oliveira, F., Cruz, G., Barbosa, M., Junior, F., Lima, R., & Gómez-Malagón, L. (2024). A proposal for a solar position sensor system with multifiber optical cable. *Sensors, 24*(11). https://doi.org/10.3390/s24113269

Osman, A. I., Chen, L., Yang, M., & others. (2022). Cost, environmental impact, and resilience of renewable energy under a changing climate: A review. *Environmental Chemistry Letters, 21*(2). https://doi.org/10.1007/s10311-022-01532-8

Pathare, A. A., & Sethi, D. (2024). Development of IoT-enabled solutions for renewable energy generation and net-metering control for efficient smart home. *Discover Internet of Things, 4*(1). https://doi.org/10.1007/s43926-024-00065-6

Ponce-Jara, M. A., Velásquez-Figueroa, C., Reyes-Mero, M., & Rus-Casas, C. (2022). Performance comparison between fixed and dual-axis sun-tracking photovoltaic panels with an IoT monitoring system in the coastal region of Ecuador. *Sustainability, 14*(3). https://doi.org/10.3390/su14031696

Rabaia, M. K. H., Abdelkareem, M. A., Sayed, E. T., & others. (2021). Environmental impacts of solar energy systems: A review. *Science of the Total Environment, 754*. https://doi.org/10.1016/j.scitotenv.2020.141989

Rao, C. K., Sahoo, S. K., & Yanine, F. F. (2023). An IoT-based intelligent smart energy monitoring system for solar PV power generation. *Energy Harvesting and Systems, 11*(1). https://doi.org/10.1515/ehs-2023-0015

Solís-Cervantes, C. U., Palomino-Resendiz, S. I., Flores-Hernández, D. A., Peñaloza-López, M. A., & Montelongo-Vazquez, C. M. (2024). Design and implementation of extremum-seeking control based on MPPT for dual-axis solar tracker. *Mathematics, 12*(12). https://doi.org/10.3390/math12121913

Vimal, V. (2024). Enhanced solar tracking system utilizing IoT for optimal energy. In *2024 2nd International Conference on Sustainable Computing and Smart Systems (ICSCSS)*. https://doi.org/10.1109/icscss60660.2024.10625348

Waldron, N., Smith, S., & Karthik, V. (2023). Solar tracking system utilizing IoT technologies for enhanced power generation. In *2023 12th International Conference on Renewable Energy Research and Applications (ICRERA)* (pp. 269–272). https://doi.org/10.1109/ICRERA59003.2023.10269398

Yang, L. Z., Yunus, M. A. M., Sahlan, S., & Jamali, A. (2023). Automated dual-axis solar tracking system using fuzzy logic control. In *2023 IEEE 9th International Conference on Smart Instrumentation, Measurement and Applications (ICSIMA)* (pp. 150–154). https://doi.org/10.1109/ICSIMA59853.2023.10373468

Zhao, X., Shen, Z., & Jing, Z. (2022). Application of wireless sensor network data fusion technology in mechanical fault diagnosis. *Mathematical Problems in Engineering, 2022*. https://doi.org/10.1155/2022/5707210